Agricultural and Forest Meteorology 322 (2022) 109026

Contents lists available at ScienceDirect

Agricultural and Forest Meteorology

journal homepage: www.elsevier.com/locate/agrformet

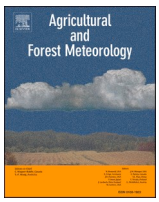

Senescence in temperate broadleaf trees exhibits species-specific dependence on photoperiod versus thermal forcing

Minkyu Moon [a,*], Andrew D. Richardson [b,c], John O'Keefe [d], Mark A. Friedl [a]

[a] Department of Earth and Environment, Boston University, USA
[b] School of Informatics, Computing, and Cyber Systems, Northern Arizona University, USA
[c] Center for Ecosystem Science and Society, Northern Arizona University, USA
[d] Harvard Forest, Harvard University, USA

ARTICLE INFO

Keywords:
Leaf senescence
Temperate deciduous forests
Photoperiod
Temperature sensitivity
Bayesian
Hierarchical modeling

ABSTRACT

Incomplete understanding of the processes controlling senescence limits our ability to forecast how the timing of leaf senescence will change in coming decades. In this study, we use a hierarchical Bayesian model (HBM) in association with a 27+ year record of field observations for 12 temperate deciduous tree species collected at Harvard Forest in central Massachusetts to examine how variability in bioclimatic controls affects the timing of leaf senescence. To test how general and extensible our results are over a broader biogeographic range, we used a multi-year record of land surface phenology derived from remote sensing encompassing all forested lands in New England. Results from the HBM showed that while air temperature is an important factor that influences the timing of leaf senescence, photoperiod uniformly exerts the strongest control across all 12 species. Species exhibiting the strongest dependence on photoperiod, particularly *Acer* species, showed low inter-annual variation and no long-term trends in the timing of leaf senescence. In contrast, species with greater dependence on air temperature, particularly *Quercus* species, showed statistically significant trends toward later senescence dates in response to long-term warming. Results from analyses conducted at regional scale across all of New England using data derived from remote sensing corroborated results obtained at Harvard Forest. Specifically, relative to ecoregions dominated by *Quercus* species, the timing of leaf senescence in ecoregions dominated by *Acer* species exhibited lower interannual variability and lower correlation with year-to-year variation in pre-senescence period mean air temperatures. These results suggest that forecasting how the timing of leaf senescence in temperate forests will change in the future requires species-specific understanding of how bioclimatic forcing controls the timing of leaf senescence.

1. Introduction

The seasonality of vegetation activity influences a wide array of ecosystem functions (Bonan, 2008). Hence, understanding how ecological and bioclimatic processes control vegetation phenology is critical to understanding how ecosystems will respond to future climate change (Buermann et al., 2018; Piao et al., 2019; Richardson et al., 2018). However, despite extensive efforts devoted to this topic, mechanistic understanding of what controls plant phenology remains incomplete (Delpierre et al., 2016; Zohner et al., 2016). In this context, a large proportion of phenological research has focused on the mechanisms that control the timing of leaf emergence, while understanding of the eco-physiological processes that control leaf senescence is less well-developed (Chen et al., 2020; Vitasse et al., 2021; Zani et al., 2020).

A key challenge in developing comprehensive understanding and models of fall phenology is that, unlike in spring, senescence is preceded by a growing season that typically spans several months. Hence, the mechanisms and processes that control leaf senescence are potentially more complex than those controlling spring phenology, which increases the challenges involved in understanding of how senescence will respond to ongoing climate change. For example, previous studies have suggested that both genetic factors (Friedman et al., 2011) and changes in bioclimatic variables throughout the growing season influence the timing of senescence (Bigler and Vitasse, 2021; Chen et al., 2020; Wu et al., 2018; Zhang et al., 2020b). Variation in the timing of leaf senescence impacts seasonal-scale ecosystem productivity by regulating the

* Corresponding author at: 685 Commonwealth Avenue, Boston, MA 02215, USA.
E-mail address: moon.minkyu@gmail.com (M. Moon).

https://doi.org/10.1016/j.agrformet.2022.109026
Received 3 February 2022; Received in revised form 9 May 2022; Accepted 23 May 2022
Available online 29 May 2022

length of growing season (Park et al., 2016; Zani et al., 2020) and nutrient status of individual trees and at the ecosystem-scale (Dox et al., 2020; Havé et al., 2017), and can also affect important ecological processes such as the timing of reproduction for many plant and animal species (Gallinat et al., 2015; Renner and Zohner, 2018). Therefore, improved understanding of the processes that control leaf senescence is needed to understand how vegetation phenology will change in the coming decades and to improve forecasts of how ecosystem functions that are affected by leaf senescence will be impacted by these changes.

The two bioclimatic factors that are most widely assumed to control the timing of leaf senescence are air temperature and day-length (i.e., photoperiod), both of which tend to decrease prior to leaf senescence in extra-tropical ecosystems (Fu et al., 2018; Gill et al., 2015; Keskitalo et al., 2005; Lang et al., 2019; Liu et al., 2020). As a result, most models use air temperature and photoperiod as the primary drivers of leaf senescence (Peano et al., 2021). In recent years, a variety of research has identified a suite of additional factors that may influence the timing of senescence including the rate and amount of photosynthesis prior to senescence onset (Zani et al., 2020), water stress (Peng et al., 2019; Xie et al., 2018), the timing of leaf emergence in spring (Keenan and Richardson, 2015; Peng et al., 2021), and plant and soil nutrient status (Estiarte and Peñuelas, 2015; Keskitalo et al., 2005). Further, several recent studies have reported that daily minimum and maximum air temperatures may have differing influence on the timing of leaf senescence (Meng et al., 2020; Wu et al., 2018). However, there is no current consensus regarding how environmental drivers control the onset of leaf senescence in temperate broadleaf forests.

A key quandary from previous studies, that has been known for nearly a decade, is that results from lab- and field-based experimental studies that have been explicitly designed to identify phenological sensitivity to climate forcing differ from patterns observed in natural ecosystems arising from climate variability (Leuzinger et al., 2011; Primack et al., 2015; Vitasse et al., 2014; Wolkovich et al., 2012; but see Hänninen et al., 2019). Further, the limited spatial and temporal coverage of these studies, which are generally conducted at local scales with study areas less than 10 km^2 and time scales shorter than 10 years, is a significant limitation that inhibits their ability to provide general results. As a solution, process-based phenological models calibrated to both *in-situ* and remote sensing-based observations of phenology have been widely used to make inferences and advance understanding of the ecological and environmental factors that control phenological events such as the start of senescence (Delpierre et al., 2009; Lang et al., 2019; Liu et al., 2020; Schaber and Badeck, 2003). Unfortunately, however, the models used in these studies include two fundamental limitations: (1) they prescribe functional relationships among forcing variables and phenological events based on incomplete understanding; and (2) the most widely-used functional forms of these models use parameters that have been aggregated over time periods that span weeks-to-months (e.g., growing degree days) and do not capture short-term variability that is increasingly recognized to have a significant impact on phenological behavior (Clark et al., 2014b; Moon et al., 2021b).

To address both the knowledge gaps and limitations of models described above, and specifically focusing on how environmental drivers control the timing of leaf senescence in temperate forests, here we use a data-driven hierarchical Bayesian model (HBM) estimated using long-term field measurements of bioclimatic forcing and leaf senescence dates for 12 temperate deciduous tree species in New England. To compare our results against a state-of-the-art process-based model, we also tested the model described by Caffarra et al. (2011), which incorporates the effects of photoperiod, air temperature, and anomalies in the timing of leaf unfolding. Using these models, we assessed their ability to explain species-specific differences in the sensitivity of fall phenology to climate forcing. To evaluate our results and conclusions at a broader geographic scale, we linked the site-level and species-specific patterns that we estimate using the HBM to regional-scale patterns and trends in the timing of senescence of temperate forests across all of New England using species density maps and large-scale records of land surface phenology from remote sensing.

2. Methods and data

2.1. Field observations

Phenological observations of woody plants have been recorded since 1990 to the present at the Harvard Forest, a long-term ecological research site located in Petersham Massachusetts (42.53° N, 72.18° W; Fig. S1) (O'Keefe, 2019). Each of the trees included in the survey is located within 1.5 km of the Harvard Forest headquarters at elevations between 335 and 365 m above sea level. For fall phenology, weekly observations of percent leaf coloration and percent leaf fall are recorded from the beginning of September to the end of leaf fall each year. In this study, we used data characterizing the timing of leaf coloring for 12 species, all of which have at least 20 years of observations over the 28 year period from 1992 to 2019 (*Acer pensylvanicum* (ACPE), *Acer rubrum* (ACRU), *Acer saccharum* (ACSA), *Amelanchier alnifolia* (AMAF), *Betula alleghaniensis* (BEAL), *Betula lenta* (BELE), *Betula papyrifera* (BEPA), *Fraxinus americana* (FRAM), *Prunus serotina* (PRSE), *Quercus alba* (QUAL), *Quercus rubra* (QURU), and *Quercus velutina* (QUVE); Table S1). Leaf coloring date is defined as the day of year (DOY) on which 50% of the leaves have changed color on an individual tree. Typically, three to five individuals of each species are observed in each year, with different individuals observed in different years (Table S2). Our analysis also used budburst date for the same trees, which is defined as the DOY when 50% of the buds on the tree have recognizable leaves emerging from them (see Section 2.3). Sub-weekly observations would be useful to help resolve rapidly changing phenological processes (e.g., Gao et al., 2017; Keenan et al., 2014). However, numerous studies have used these data to estimate models and analyze trends in phenology at Harvard Forest (e.g., Archetti et al., 2013; Dunn et al., 2021; Richardson et al., 2006), which demonstrates that these data provide a sound basis for phenological studies. Measurements of carbon fluxes and daily meteorology were obtained from the Harvard Forest Environmental Monitoring Station (EMS) eddy covariance tower (Munger and Wofsy, 2020).

2.2. Modeling long-term trends in leaf senescence

In the first element of our analysis, we estimated species-specific long-term trends in the timing of leaf senescence. To do this, we used the non-parametric Theil-Sen estimator to estimate the trend for each tree species (Sen, 1968), and distinguished species with statistically significant trends ($p < 0.05$) from those not showing trends using the Mann-Kendall test (Mann, 1945). We also estimated long-terms trends in air temperatures measured at the EMS tower using the same approach for each of annual, late summer (from August to October; i.e., directly prior to leaf senescence), and spring (from March to May) time periods.

2.3. Hierarchical Bayesian model of leaf senescence

To estimate the sensitivity of leaf senescence timing to bioclimatic controls, we used a hierarchical Bayesian model (HBM) estimated using the field observations described in Section 2.1. The original form of this model was proposed by Clark et al. (2014b, 2014a), and Moon et al. (2021b) recently adapted it to model springtime phenology at large spatial scale using remote sensing. The HBM has two main advantages for the analysis we describe here. First, because the relative importance among bioclimatic controls that affect the timing of senescence is estimated by data itself, the HBM does not suffer from issues related to model misspecification related to prescribed functional relationships among control variables that are embedded in conventional process-based models (see Peano et al. (2021) and Section 2.4). Second, the HBM is estimated using daily data and so is able to capture the continuous response of phenological processes to both short- and

long-term variation in environmental forcing (Clark et al., 2014b, 2014a; Moon et al., 2021b).

The HBM uses a state-space framework that includes an unobserved latent state h to continuously track the response of phenological processes to environmental forcing at daily time step. In this framework, changes in the latent state (h) are computed as:

$$h_{d+1} = h_d + \delta h_d \tag{1}$$

where h_d is the latent state on day d. δh_d is the change in h from day d to day $d+1$, which is estimated as:

$$\delta h_d = \begin{cases} (X_d\beta)(1 - h_d/h_{max}), & \delta h_d \geq 0 \\ 0, & \delta h_d < 0 \end{cases} \tag{2}$$

where X_d is a matrix of predictors that includes daily meteorological forcing variables (air temperature, photoperiod, vapor pressure deficit (VPD), and photosynthetically active radiation (PAR)), along with species-specific budburst dates and early-season gross primary productivity (GPP) derived from eddy covariance measurements at the Harvard Forest EMS tower. Here, we define early-season GPP as the accumulated daily GPP from May 1 to July 31, which nominally corresponds to the first half of the growing season. β is a vector of estimated model coefficients (i.e., posterior distributions from the model). Note that because the input data (X_d) are normalized (i.e., to have a mean of 0 and a standard deviation of 1 for each of the input variables) prior to model estimation, the magnitudes of each model coefficient, which reflect the dependence of senescence development on each input variable (i.e., β), are independent of the magnitude and units of each input variable (and hence can be compared). h_{max} is the final state value of h, and is prescribed to be 100.

To link the continuous scale of the latent state h to a form that identifies discrete phenological events (*i.e.*, recorded dates of leaf senescence), we use a logit transformation:

$$logit(P_d) = \kappa + \lambda \times h_d \tag{3}$$

where P_d is the probability that leaf senescence occurs on day d, and κ and λ are the intercept and slope of the transformation, respectively. Because the leaf senescence date is defined to be a discrete event, P_d follows a Bernoulli distribution:

$$Y_d \sim Bernoulli(P_d) \tag{4}$$

where Y_d indicates whether leaf senescence has occurred on day d (i.e., 1 or 0).

2.4. Model estimation and evaluation

To estimate the HBM, we used the median date of leaf senescence in each year from observations of 3 to 5 individual trees, which yielded a 28-year time series of leaf senescence dates for each species except QURU, which had a 27-year record (Table S2). Using these data, we estimated the HBM for six different sets of bioclimatic variables with two main goals: (1) to quantify the relative importance of each variable in controlling in the timing of leaf senescence; and (2) to assess whether daily minimum and maximum air temperatures have distinct roles in controlling the timing of leaf senescence relative to mean daily temperature (see Meng et al., 2020 and Wu et al., 2018). To this end, we estimated six distinct HBMs using different combinations of (1) daily mean air temperature, (2) daily minimum air temperature, (3) daily maximum air temperature, (4) daily minimum and maximum air temperatures, and (5) daily mean air temperature and daily temperature range, along with photoperiod, VPD, PAR, species-specific budburst dates, and early-season GPP as predictor variables (hereafter, models M1-M5, respectively). Further, to assess the role and importance of photoperiod in controlling the timing of leaf senescence, we estimated the HBM using daily mean air temperature with all other variables, excluding photoperiod (model M6). Each models' performance was evaluated based on the root-mean-square error (RMSE), mean absolute error (MAE), and deviance information criterion (DIC). Posterior sampling was performed using the 'R2jags' package in R (Su and Yajima, 2015), with 10,000 iterations and 3000 burn-in periods for each model.

In addition, to evaluate the HBM's performance against a state-of-the-art of process-based leaf senescence model, we used the Harvard Forest data set to estimate the model described by Caffarra et al. (2011) (hereafter CSM). We chose the CSM for this comparison based on recent results from Liu et al. (2020), who used multiple widely used process-based leaf senescence models in association with over 19,000 site-years of *in-situ* phenological records covering four temperate deciduous tree species in Europe to show that the CSM performed best among the models they used, especially in capturing interannual variation in leaf senescence dates. The CSM hypothesizes that the progression of leaf senescence, which is defined as the dormancy induction state DS, is negatively related to both air temperature and photoperiod via sigmoidal relationships. Specifically, daily accumulation of DS is controlled by air temperature and photoperiod as follows:

$$DS(d) = \sum_{d_0}^{d} \frac{1}{1 + e^{aD\left(T_{(d)} - bD\right)}} \times \frac{1}{1 + e^{cD\left(P_{(d)} - P_{crit}\right)}} \tag{5}$$

where d_0 is the start date of dormancy induction, which we prescribed as September 1st, and aD, bD, and cD are model coefficients. Leaf senescence occurs when the accumulated forcing (i.e., $DS(d)$) reaches a critical threshold D_{crit}, which is a function of the anomaly in springtime phenology S_a:

$$D_{crit} = \alpha + \gamma \times S_a \tag{6}$$

where α and γ are parameters regulating the effects of changes in springtime phenology. For this study, we used the budburst dates collected at Harvard Forest as a proxy of springtime phenology. Parameters were optimized to minimize the RMSE in predicted versus observed senescence dates for each of the 12 species following the method described by Nelder and Mead (1965).

Lastly, to assess how the relative dependence on photoperiod versus air temperature (i.e., the two dominant factors controlling in the timing of leaf senescence; see the Results) estimated by the HBM affect year-to-year variation in the timing of leaf senescence, we calculated the difference between the posterior distributions of photoperiod and air temperature (i.e., $\beta_P - \beta_T$) for each species ($n = 12$), and used standard major axis regression to assess the magnitude of covariance between $\beta_P - \beta_T$ and interannual variation in leaf senescence dates.

2.5. Remote sensing data

To expand and generalize our analysis to regional scale, we used Version 1.1 of the Multi-Source Land Surface Phenology product (MSLSP30NA) (Friedl, 2021). This data product provides yearly observations of phenophase transition dates at 30 m spatial resolution for North America for 2016–2020. Using time series of the two-band enhanced vegetation index (EVI2; Jiang et al., 2008) estimated from Harmonized Landsat 8 and Sentinel-2 (HLS) imagery (Claverie et al., 2018), the MSLSP30NA product retrieves the timing of seven phenophase transition dates for each growing season at each 30 m pixel (Bolton et al., 2020). To identify the timing of leaf senescence we used the MSLSP30NA mid-greendown date, which corresponds to the DOY when EVI2 time series pass below 50% of the EVI2 amplitude during the greendown phase. More specifically, we used mid-greendown dates for all deciduous broadleaf or mixed forest pixels in New England according to the 2016 USGS National Land Cover Database (USGS and Rigge, 2019), which includes 40 Level IV EPA ecoregions (Fig. S1).

We used the MSLSP30NA data set to perform two analyses designed to assess whether species-specific results obtained from *in-situ*

observations at Harvard Forest generalize at regional scale. First, because the remote sensing time series is short and it is computationally infeasible to run the HBM at every pixel in New England, we examined the relationship between anomalies in the timing of senescence dates and mean air temperature in the pre-senescence period, which we defined as DOY 231 to 270 based on results from the HBM at Harvard Forest (Fig. S2). Second, we calculated the standard deviation (SD) in the timing of senescence at each 30-m pixel across the available time series for all forested pixels in New England. Using these data, we estimated a multiple linear regression using the basal area for *Acer* and *Quercus* species in each ecoregion as independent variables (i.e., the total basal area for all three species for each of *Acer* and *Quercus* in each EPA ecoregion) and the standard deviation of senescence dates across years in each ecoregion as the dependent variable. For the species-specific basal areas, we used a gridded dataset provided by the USDA Forest Service derived from satellite imagery in conjunction with extensive field plot data providing tree species basal area (Wilson et al., 2013).

3. Results

Since 1992, annual mean air temperature at Harvard Forest has increased by 0.034 °C per year ($p = 0.035$), resulting in a total increase of 0.95 °C over the past 30 years (Fig. S3a). During late summer, when the impact of changes in bioclimatic variables on the timing of leaf senescence is most pronounced (Fig S2), the warming trend was even stronger (0.059 °C per year; Fig. S3b). Inspection of long-term trends in the timing of senescence in response to this warming indicates that the response of trees was species-specific (Fig. 1). Specifically, four of the twelve species included in our analysis showed statistically significant trends towards later senescence onset dates (QUVE, QURU, PRSE, and ACPE (see Fig. 1 for full species names); p-value < 0.05), with trends that range from 0.18 days per year to 0.30 days per year, corresponding to a total shift of 5.0–8.4 days towards later onset of senescence dates over the 28-year study period. Among the species showing non-significant trends, five species (ACRU, BEAL, BELE, PRSE, and QUAL) showed positive trends (i.e., later senescence), two species (ACSA and BEPA) showed negative trends, and one species (AMAF) showed no trend. These results identify species-specific responses to identical bioclimatic forcing over three decades,.

We tested six versions of the HBM using different combinations of bioclimatic predictor variables (Table 1). Overall, RMSEs and MAEs were low (ranging from 2.84 to 5.15 days and from 2.21 to 4.14 days, on average, respectively), suggesting that the models realistically capture the eco-physiological response of deciduous trees to bioclimatic forcing during the leaf senescence phase. Among the different models, M5, which uses daily mean air temperature and daily air temperature range as predictors along with all the other variables, exhibited the best performance across all three model performance metrics. It is worth noting that model M6, which does not include photoperiod as a predictor,

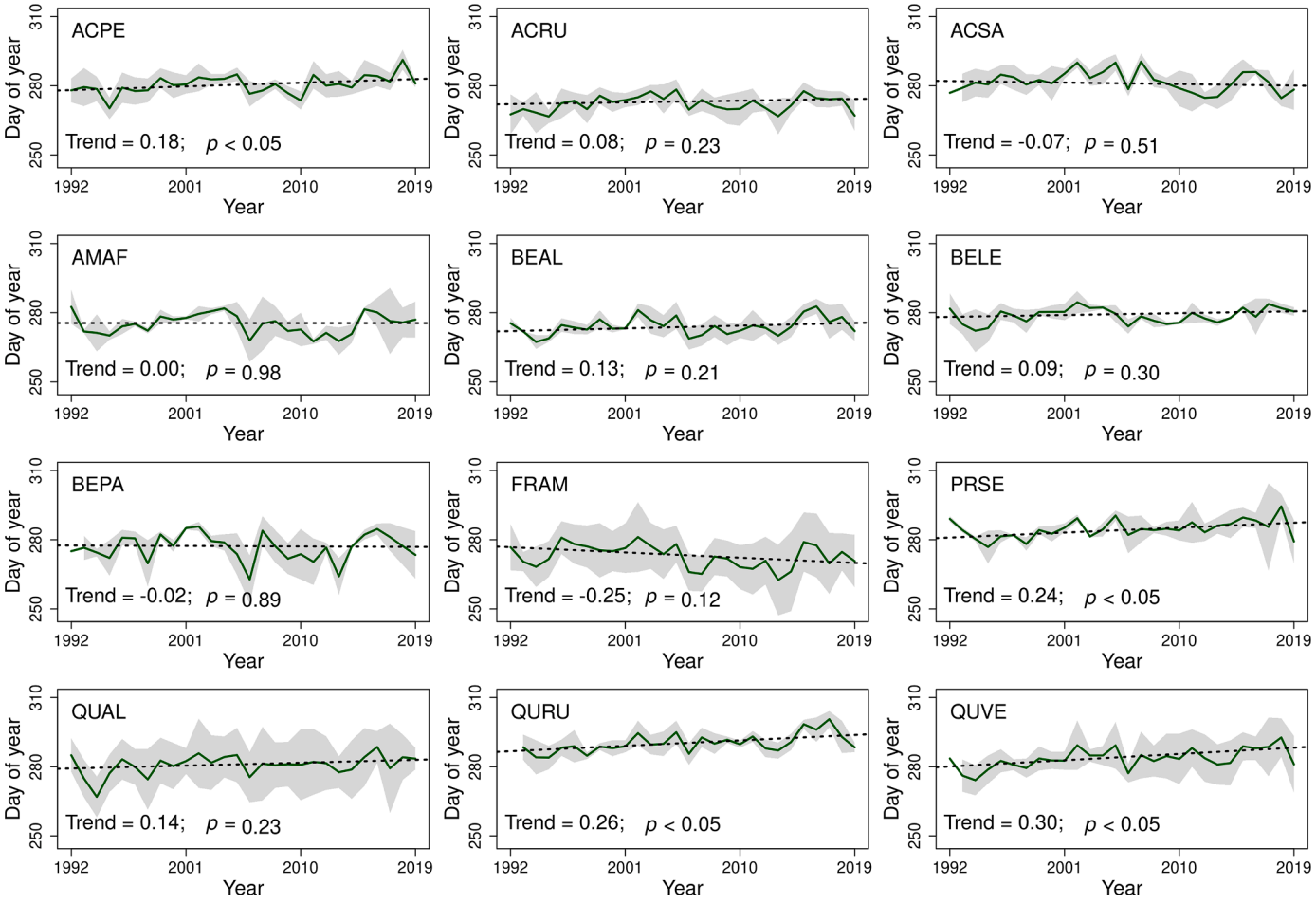

Fig. 1. Leaf coloration dates at Harvard Forest from 1992 to 2019. Solid green lines and shaded areas represent the annual mean and standard deviation in leaf coloration dates, respectively. Black dashed lines show the long-term trend (based on the Theil-Sen estimator) in days per year. APCE: *Acer pensylvanicum*; ACRU: *Acer rubrum*; ACSA: *Acer saccharum*; AMAF: *Amelanchier alnifolia*; BEAL: *Betula alleghaniensis*; BELE: *Betula lenta* BEPA: *Betula papyrifera*; FRAM: *Fraxinus americana*; PRSE: *Prunus serotina*; QUAL: *Quercus alba*; QURU: *Quercus rubra*; QUVE: *Quercus velutina.* (For interpretation of the references to color in this figure legend, the reader is referred to the web version of this article.).

Table 1
Hierarchical Bayesian model performance statistics. M1-M6 refer to models using different sets of predictors: models M1-M5 use daily mean air temperature, daily minimum air temperature, daily maximum air temperature, daily minimum and maximum air temperatures, and daily mean air temperature and daily temperature range as predictor variables, along with photoperiod, vapor pressure deficit, photosynthetically active radiation, species-specific budburst dates, and early-season gross primary productivity; model M6 uses daily mean air temperature and includes all other variables except photoperiod. RMSE: root-mean-square error; MAE: mean absolute error; DIC: deviance information criterion. See Fig. 1 for definitions of species acronym.

Species	RMSE						MAE						DIC					
	M1	M2	M3	M4	M5	M6	M1	M2	M3	M4	M5	M6	M1	M2	M3	M4	M5	M6
ACPE	2.76	2.38	3.21	2.32	2.35	4.87	2.04	1.86	2.29	1.82	1.79	4.04	284	256	329	252	251	525
ACRU	2.54	2.55	2.83	2.61	2.48	5.57	1.89	1.93	2.11	1.96	1.93	4.64	285	278	298	280	281	592
ACSA	3.83	3.86	3.96	3.77	3.90	6.43	3.11	3.04	3.29	2.96	3.11	5.14	415	417	416	420	419	638
AMAF	3.15	3.23	3.23	3.27	3.08	5.22	2.46	2.86	2.46	2.61	2.46	4.21	335	343	344	342	336	534
BEAL	2.19	2.04	2.48	2.04	1.98	4.77	1.79	1.64	2.07	1.68	1.57	4.00	234	209	264	211	217	478
BELE	2.10	2.35	2.35	2.21	2.08	4.40	1.57	1.61	1.96	1.61	1.54	3.57	241	249	261	246	245	476
BEPA	4.90	4.62	5.04	4.80	4.73	6.18	3.89	3.61	4.07	3.61	3.54	4.82	502	486	519	489	493	655
FRAM	3.52	3.51	3.71	3.52	3.45	6.32	2.96	2.93	3.04	2.86	2.75	4.75	385	365	395	389	375	622
PRSE	2.57	2.57	2.71	2.54	2.58	5.07	2.18	2.04	2.18	2.04	2.07	3.86	278	318	293	333	275	516
QUAL	2.66	2.92	2.76	2.72	2.66	4.85	1.93	2.18	2.14	2.04	1.93	3.89	291	306	303	293	293	494
QURU	2.59	2.43	2.69	2.53	2.45	3.98	2.04	1.96	2.15	2.04	2.00	3.33	263	257	277	260	263	403
QUVE	2.45	2.46	2.62	2.41	2.41	4.13	1.79	1.86	2.07	1.68	1.82	3.43	272	347	285	366	272	428
Average	2.94	2.91	3.13	2.90	**2.84**	**5.15**	2.30	2.29	2.49	2.24	**2.21**	**4.14**	315	319	332	323	**310**	**530**

showed substantially worse predictive accuracy relative to the other five models. Scatterplots showing modeled versus observed leaf senescence dates provide visual corroboration that the HBM accurately predicts the observed timing of leaf senescence across all 12 species and demonstrates that the HBM predicts interannual variation in the timing of senescence (e.g., QURU) with substantially more accuracy and realism than the CSM for all 12 species (Fig. 2 and Table S3). Based on these results, hereafter we use model M5 for the rest of our analyses.

Results from the HBM indicate that air temperature and photoperiod are the two most important factors that control the timing of senescence (Fig. 3). Significantly, however, and consistent with results presented above examining long term trends in the timing of senescence, HBM results also show that the relative dependence of senescence on each of these controls is species-specific. Negative dependences indicate that decreases in the forcing variable prior to leaf senescence increase the probability of senescence. Hence, stronger negative dependence on air temperature and photoperiod relative to other variables reflect the fact that seasonal variation in air temperature and photoperiod (i.e., cooling and shorter day-length, respectively) are the dominant factors that control the timing of leaf senescence. Relative to air temperature and photoperiod, the impact of the other variables included in the model (daily range of air temperature, VPD, PAR, budburst dates, and spring GPP) is modest. In this context, two key features are worth noting. First, across all 12 species, dependence on photoperiod is stronger than dependence on air temperature. Second, even though its overall effect is quite modest, the timing of leaf senescence exhibits mostly positive dependence on daily air temperature range, suggesting that larger amplitudes in daily air temperature promote earlier leaf senescence dates.

Covariation between the magnitude of interannual variation in leaf senescence dates and differences in the magnitude of photoperiod (β_P) and air temperature (β_T) dependence shows strong correlation (Fig. 4). This result provides additional empirical evidence that stronger species-specific dependence on photoperiod (air temperature) leads to smaller (larger) interannual variation in leaf senescence dates. For example, on average, *Acer* species, which show larger photoperiod dependence compared to other species, exhibit lower magnitudes of interannual variation in senescence dates, whereas *Quercus* species, which show the weakest dependence on photoperiod (i.e., relatively greater dependence on temperature compared to *Acer* species), exhibit larger magnitudes of interannual variation.

Land surface phenology data from remote sensing capture geographic patterns in the timing of leaf senescence at regional scale that are consistent with species-level patterns at Harvard Forest shown in Fig. 4 (Fig. 5). Specifically, eco-regions in New England where *Acer* species are more abundant show lower interannual variability in the timing of leaf senescence relative to areas dominated by *Quercus* species

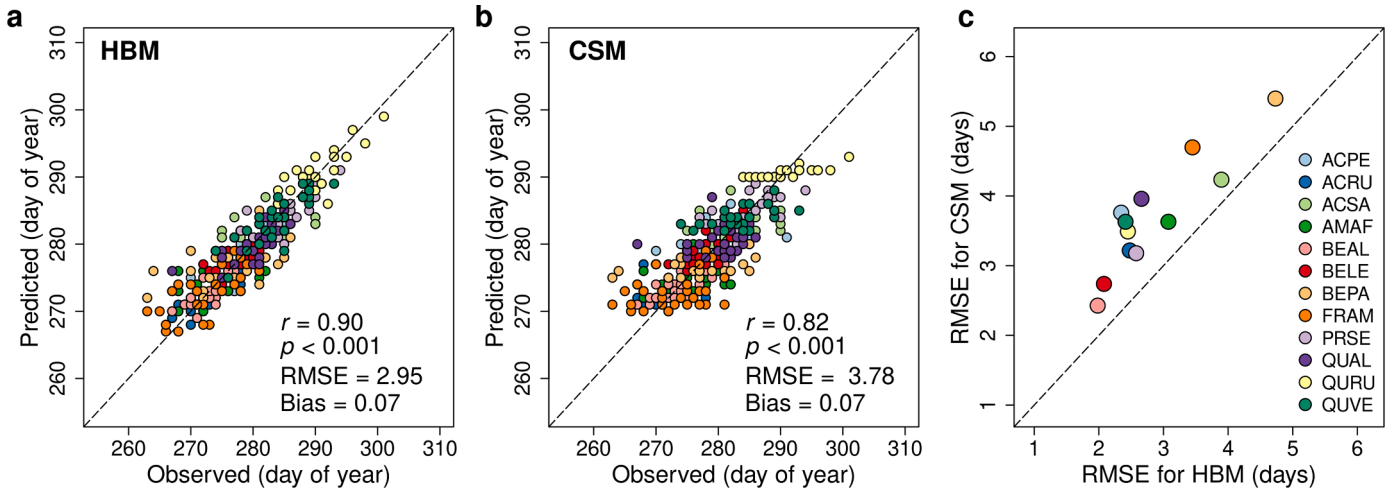

Fig. 2. Observed versus predicted leaf senescence dates across 12 deciduous tree species from (a) the Hierarchical Bayesian Model of leaf senescence and (b) the CSM model, and (c) comparison of RMSE's from each model. See Fig. 1 for definitions of species acronyms.

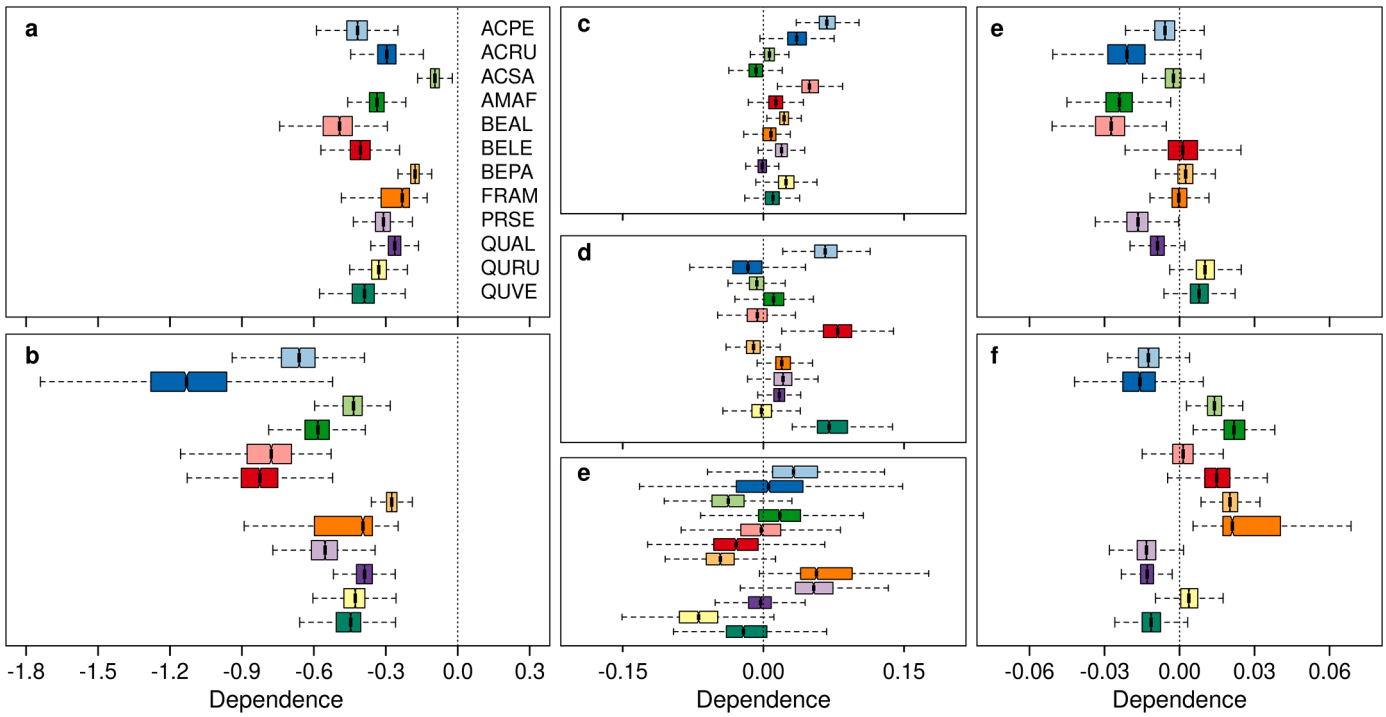

Fig. 3. Dependence of leaf senescence date on (a) daily mean air temperature, (b) photoperiod, (c) daily range in air temperature, (d) daily mean vapor pressure deficit, (e) daily mean photosynthetically active radiation, (f) budburst dates, and (g) early-season gross primary productivity. Note that the magnitude of dependence in each column is different and decreases from left to right. See Fig. 1 for definitions of species acronym.

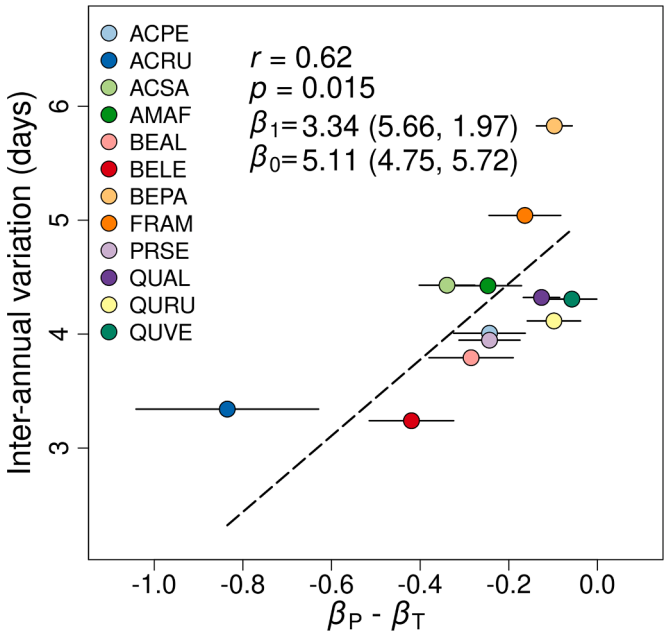

Fig. 4. Relationship between interannual variation in the timing of leaf senescence and the difference between photoperiod (β_P) and air temperature (β_T) dependence estimated by the HBM. The points and horizontal bars present the median ± one standard deviation, respectively, in the posterior distributions. The dashed line shows the standard major axis regression (SMA). SMA slope (β_1) and intercept (β_0) coefficients are provided with 95% confidence intervals. See Fig. 1 for definitions of species acronyms.

(Figs. 5a and S4a). Further, *Quercus*-dominant regions showed greater sensitivity to pre-senescence period mean air temperature (i.e., stronger dependence on air temperature), while *Acer*-dominant regions showed weaker sensitivity (Figs. 5b and S4b). Reinforcing this, results from a multiple linear regression using the basal area of *Acer* and *Quercus* species as predictors explained 63% of interannual variation in the timing of leaf senescence across the 40 EPA Level IV ecoregions in New England (Fig. 5d).

4. Discussion

4.1. Bioclimatic controls on leaf senescence

Consistent with previous studies, results from this work support the argument that air temperature and photoperiod are the dominant factors that control the timing of leaf senescence (Archetti et al., 2013; Fracheboud et al., 2009; Gill et al., 2015; Lang et al., 2019; Liu et al., 2020; Vitasse et al., 2021; Zhang et al., 2020a). However, by quantifying the relative importance among a large suite of bioclimatic controls using a data-driven HBM, we demonstrate that the relative influence of photoperiod and air temperature far exceed the influence of all other bioclimatic controls, and that photoperiod was the most influential control across all 12 deciduous tree species considered in this study. Indeed, excluding photoperiod as a predictor in the HBM substantially degraded the accuracy of model predictions (models M1-M5 versus model M6 in Table 1). Moreover, given the structure of the HBM, which tracks continuous development of leaf senescence at daily time step, our results indicate that the influence of photoperiod on the timing of senescence occurs over an extended period prior to senescence onset. Stated another way, photoperiod exerts continuous forcing that acts in concert with other forcing variables (primarily temperature) and does not simply act as a trigger that initiates senescence after a species-specific threshold is reached. Recent studies using process-based models incorporating a continuous effect of photoperiod (with joint control from air temperature) have reported that these models perform better than process-based models that use photoperiod as a cue (Lang et al., 2019; Liu et al., 2020), which supports our findings.

More generally, by using the HBM to test different sets of bioclimatic controls, results from this study provide useful insights to recent debates

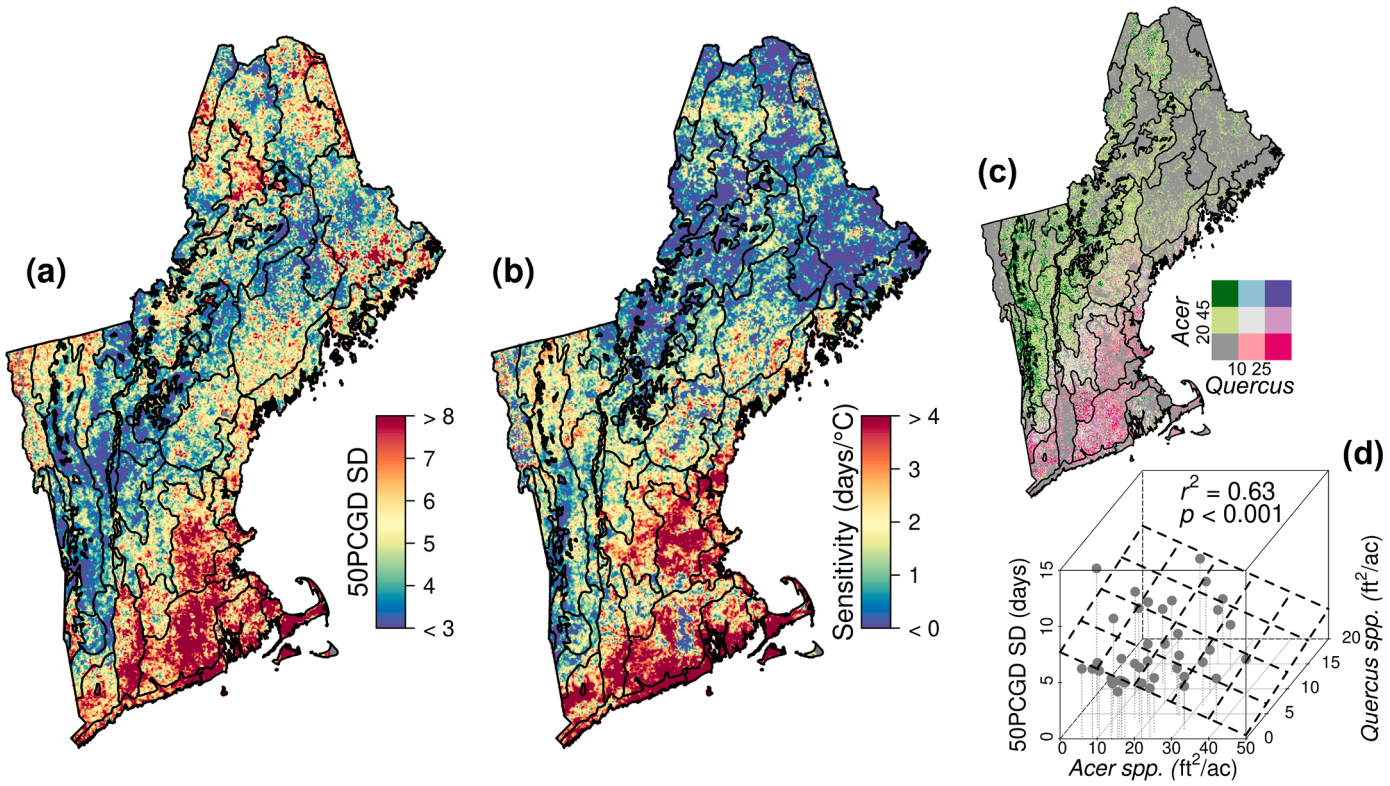

Fig. 5. Geographic variation in (a) the standard deviation (SD) of mid-greendown dates derived from 30 m spatial resolution HLS imagery from 2016 to 2020, (b) sensitivity to pre-senescence period mean air temperature, and (c) basal area for *Acer* and *Quercus* species. Panel (d) shows results from a multiple linear regression demonstrating that 63% of geographic variation in the magnitude of ecoregion-scale interannual variation in senescence onset dates from remote sensing is explained by the basal area of *Acer* and *Quercus* species in each EPA Level IV ecoregion (n = 40).

regarding the representation of thermal forcing in senescence models (e.g., the role of mean versus minimum versus maximum air temperature; see Meng et al., 2020 and Wu et al., 2018). Specifically, results from the HBM show that daily mean air temperature and the daily range in air temperatures is the most effective combination of thermal forcing variables for predicting the timing of senescence (Table 1), and that larger amplitudes in daily air temperature lead to earlier leaf senescence (Fig. 3c). These results may support the argument that minimum and maximum air temperatures have distinct roles in controlling the timing of leaf senescence (specifically, that higher maximum temperatures lead to earlier leaf senescence, while higher daily minimum temperature lead to later leaf senescence; Wu et al., 2018). However, given that the overall impact of temperature range is relatively modest (as well as the high correlation between daily minimum and maximum temperature), these results should be viewed as a justification for more research rather than definitive evidence.

Significantly, outside of photoperiod and air temperature, none of the forcing variables consistently exerted a substantial influence on the timing of senescence. The dependence of daily temperature range and daily mean VPD was statistically different from zero (i.e., more than 95% of the sampled model coefficients excluded zero; Fig. 3) for only three species in each case (ACPE, BEAL, BEPA and ACPE, BELA, QUVE, respectively), and daily mean PAR was not statistically different from zero for any of the twelve species. Three species (AMAF, BEAL, and PRSE) exhibited negative dependence on the timing of budburst (i.e., earlier budburst leads to earlier senescence) and five species (ACSA, AMAF, BEPA, FRAM, and QUAL) exhibited dependence on early season GPP, with the first four of these species exhibiting positive coefficients (i.e., higher early season GPP leading to earlier leaf senescence). But, for all these latter cases, the magnitude of dependence was small. Hence, outside of photoperiod and daily mean air temperature, the sensitivity of leaf senescence to other bioclimatic forcing variables was either non-significant, or very modest and species-specific. In this context, results from the HBM do not support results from recent studies reporting that early-season GPP (Zani et al., 2020), springtime phenology (Keenan and Richardson, 2015), and VPD (Peng et al., 2021) are important controls on the timing of leaf senescence.

4.2. Implications for land surface models

Phenology exerts first-order control on a wide array of ecological functions (e.g., photosynthesis and transpiration) and surface properties (e.g., albedo) that strongly influence water, energy, and carbon exchange in land surface models (Moon et al., 2020; Piao et al., 2019; Xu et al., 2020; Young et al., 2021). Despite this, current models include only very crude (and as a result unrealistic) representation of fall phenology (Richardson et al., 2012). Most land surface models (LSMs) use air, soil, or surface temperature as a primary driver, in conjunction with secondary variables such as day-length (i.e., photoperiod), soil moisture, precipitation, and/or carbon balance, to simulate the timing of leaf senescence (Peano et al., 2021; Richardson et al., 2012). However, results from this study indicate that photoperiod is uniformly the strongest factor controlling the timing of leaf senescence, at least in temperate deciduous forests (Figs. 3 and 4). This mis-parameterization almost certainly explains why current LSMs simulate the timing of senescence so poorly. Moreover, the lower predictive power of the CSM compared to the HBM, especially in capturing interannual variation in the timing of leaf senescence (Fig. 2), implies that current process-based leaf senescence models do not realistically represent the nature and timing of leaf senescence processes. Given this, results from this work suggest that integration of data-driven phenology models, which are able to accurately represent the role of photoperiod, is a promising approach for triggering leaf senescence in the next generation of LSMs that has the potential to substantially benefit simulations of water,

energy, and carbon fluxes in these models (Reichstein et al., 2019).

A related conclusion, which also has substantial implications for representation of phenology in LSMs, is that even though all the trees at Harvard Forest experienced the same bioclimatic forcing and changes therein (i.e., warming over the last 30 years (Fig. S3)), individual species responded differently from one another. Specifically, we showed that species-specific dependence on bioclimatic controls among the 12 species examined resulted in divergent responses to climate change over nearly three decades (Fig. 1). Further, using regional-scale land surface phenology data along with stand-level species composition maps, we demonstrated that results obtained at Harvard Forest (i.e., that inter-annual variation and sensitivity to temperature and photoperiod in the timing of leaf senescence are species-specific characteristics (Fig. 5)) were robust at regional scale. Given that most LSMs classify vegetation into plant functional types and then parameterize phenology sub-models according to plant functional type, our study suggests that this approach may introduce a substantial source of model error in LSM simulation results. Hence, integrating data-driven phenology sub-models and embracing species composition maps using finer spatial satellite imagery such as HLS and perhaps PlanetScope (c.f., Hemmerling et al., 2021; Moon et al., 2021a) may provide a useful basis for improving LSM representation of fall phenology, and by extension, LSM-based simulation of water, carbon, and energy exchange.

5. Conclusions

In this study, we assessed how interannual variability in bioclimatic controls affects the timing of leaf senescence in temperate deciduous forests. To do this, we used a data-driven hierarchical Bayesian model calibrated to nearly three decades of species-specific field measurements of leaf coloration dates for 12 temperate deciduous tree species in New England. To expand and test the generality of our results, we used land surface phenology time series at 30 m spatial resolution derived from remote sensing in combination with species composition maps to show that results obtained at a single site (Harvard Forest) are consistent with the response of senescence to bioclimatic forcing at regional scale. Our results identify three important implications for understanding and modeling the timing of leaf senescence in temperate deciduous forests. First, photoperiod was uniformly more important than air temperature in controlling the timing of leaf senescence in all 12 deciduous tree species that we examined in this study. Second, the data-driven HBM outperformed the more traditional process-based CSM, especially in capturing interannual variation in the timing of leaf senescence, which reinforces the dominant role of photoperiod. Third, phenological responses to long-term trends in air temperatures were species-specific. In particular, species exhibiting stronger photoperiod dependence showed lower inter-annual variation and no trend in the timing of leaf senescence in response to the warming over the last 30 years. In contrast, species showing stronger air temperature dependence showed delayed trends in the timing of senescence that are consistent with a response to warming. Together, these results suggest that accurate forecasting of how the timing of leaf senescence will respond to future climate change requires that models account for how bioclimatic factors control the timing of leaf senescence at the species-level. Data-driven approaches such as the HBM used in this study are promising tools not only for improving models to predict the timing of leaf senescence, but more generally, for improving the representation of phenology in land surface models.

CRediT authorship contribution statement

Minkyu Moon: Conceptualization, Data curation, Formal analysis, Methodology, Visualization, Writing – original draft, Writing – review & editing. **Andrew D. Richardson:** Funding acquisition, Project administration, Writing – review & editing. **John O'Keefe:** Data curation, Writing – review & editing. **Mark A. Friedl:** Conceptualization, Funding acquisition, Project administration, Writing – original draft, Writing – review & editing.

Declaration of Competing Interest

The authors declare no competing interests.

Acknowledgments

This work was supported by NASA grant #80NSSC18K0334 and by NSF award #1702627. Additional funding, through the National Science Foundation's LTER program, supported research at Harvard Forest (DEB-1237491). A.D.R acknowledges support from DEB-1832210 and DEB-1702697.

Supplementary materials

Supplementary material associated with this article can be found, in the online version, at doi:10.1016/j.agrformet.2022.109026.

References

Archetti, M., Richardson, A.D., O'Keefe, J., Delpierre, N., 2013. Predicting climate change impacts on the amount and duration of autumn colors in a New England forest. PLoS ONE 8, e57373. https://doi.org/10.1371/journal.pone.0057373.

Bigler, C., Vitasse, Y., 2021. Premature leaf discoloration of European deciduous trees is caused by drought and heat in late spring and cold spells in early fall. Agric. For. Meteorol. 307, 108492 https://doi.org/10.1016/j.agrformet.2021.108492.

Bolton, D.K., Gray, J.M., Melaas, E.K., Moon, M., Eklundh, L., Friedl, M.A., 2020. Continental-scale land surface phenology from harmonized Landsat 8 and Sentinel-2 imagery. Remote Sensing of Environment 240, 111685. https://doi.org/10.1016/j.rse.2020.111685.

Bonan, G.B., 2008. Forests and climate change: forcings, feedbacks, and the climate benefits of forests. Science 320, 1444–1449. https://doi.org/10.1126/science.1155121.

Buermann, W., Forkel, M., O'Sullivan, M., Sitch, S., Friedlingstein, P., Haverd, V., Jain, A.K., Kato, E., Kautz, M., Lienert, S., Lombardozzi, D., Nabel, J.E.M.S., Tian, H., Wiltshire, A.J., Zhu, D., Smith, W.K., Richardson, A.D., 2018. Widespread seasonal compensation effects of spring warming on northern plant productivity. Nature 562, 110–114. https://doi.org/10.1038/s41586-018-0555-7.

Caffarra, A., Donnelly, A., Chuine, I., 2011. Modelling the timing of Betula pubescens budburst. II. Integrating complex effects of photoperiod into process-based models. Clim. Res. 46, 159–170. https://doi.org/10.3354/cr00983.

Chen, L., Hänninen, H., Rossi, S., Smith, N.G., Pau, S., Liu, Z., Feng, G., Gao, J., Liu, J., 2020. Leaf senescence exhibits stronger climatic responses during warm than during cold autumns. Nat. Clim. Change 1–4. https://doi.org/10.1038/s41558-020-0820-2.

Clark, J.S., Melillo, J., Mohan, J., Salk, C., 2014a. The seasonal timing of warming that controls onset of the growing season. Glob. Chang Biol. 20, 1136–1145. https://doi.org/10.1111/gcb.12420.

Clark, J.S., Salk, C., Melillo, J., Mohan, J., 2014b. Tree phenology responses to winter chilling, spring warming, at north and south range limits. Funct. Ecol. 28, 1344–1355. https://doi.org/10.1111/1365-2435.12309.

Claverie, M., Ju, J., Masek, J.G., Dungan, J.L., Vermote, E.F., Roger, J.-C., Skakun, S.V., Justice, C., 2018. The Harmonized Landsat and Sentinel-2 surface reflectance data set. Remote Sens. Environ. 219, 145–161. https://doi.org/10.1016/j.rse.2018.09.002.

Delpierre, N., Dufrêne, E., Soudani, K., Ulrich, E., Cecchini, S., Boé, J., François, C., 2009. Modelling interannual and spatial variability of leaf senescence for three deciduous tree species in France. Agric. For. Meteorol. 149, 938–948. https://doi.org/10.1016/j.agrformet.2008.11.014.

Delpierre, N., Vitasse, Y., Chuine, I., Guillemot, J., Bazot, S., Rutishauser, T., Rathgeber, C.B.K., 2016. Temperate and boreal forest tree phenology: from organ-scale processes to terrestrial ecosystem models. Ann. For. Sci. 73, 5–25. https://doi.org/10.1007/s13595-015-0477-6.

Dox, I., Gričar, J., Marchand, L.J., Leys, S., Zuccarini, P., Geron, C., Prislan, P., Mariën, B., Fonti, P., Lange, H., Peñuelas, J., Van den Bulcke, J., Campioli, M., 2020. Timeline of autumn phenology in temperate deciduous trees. Tree Physiol. 40, 1001–1013. https://doi.org/10.1093/treephys/tpaa058.

A, R.van der, Dunn, R.J.H., Aldred, F., Gobron, N., Miller, J.B., Willett, K.M., Ades, M., Adler, R., Richard, P.A., Allan, R., Anderson, J., Argüez, A., Arosio, C., Augustine, J. A., Azorin-Molina, C., Barichivich, J., Beck, H.E., Becker, A., Bellouin, N., Benedetti, A., Berry, D.I., Blenkinsop, S., Bock, O., Bodin, X., Bosilovich, M.G., Boucher, O., Buehler, S.A., Calmettes, B., Carrea, L., Castia, L., Christiansen, H.H., Christy, J.R., Chung, E.-S., Coldewey-Egbers, M., Cooper, O.R., Cornes, R.C., Covey, C., Cretaux, J.-F., Crotwell, M., Davis, S.M., Jeu, R.A.M.de, Degenstein, D., Delaloye, R., Girolamo, L.D., Donat, M.G., Dorigo, W.A., Durre, I., Dutton, G.S., Duveiller, G., Elkins, J.W., Fioletov, V.E., Flemming, J., Foster, M.J., Frith, S.M., Froidevaux, L., Garforth, J., Gentry, M., Gupta, S.K., Hahn, S., Haimberger, L., Hall, B.D., Harris, I., Hemming, D.L., Hirschi, M., Ho, S., Hrbacek, F., Hubert, D.,

Hurst, D.F., Inness, A., Isaksen, K., John, V.O., Jones, P.D., Junod, R., Kaiser, J.W., Kaufmann, V., Kellerer-Pirklbauer, A., Kent, E.C., Kidd, R., Kim, H., Kipling, Z., Koppa, A., Kraemer, B.M., Kratz, D.P., Lan, X., Lantz, K.O., Lavers, D., Loeb, N.G., Loyola, D., Madelon, R., Mayer, M., McCabe, M.F., McVicar, T.R., Mears, C.A., Merchant, C.J., Miralles, D.G., Moesinger, L., Montzka, S.A., Morice, C., Mösinger, L., Mühle, J., Nicolas, J.P., Noetzli, J., Noll, B., O'Keefe, J., Osborn, T.J., Park, T., Pasik, A.J., Pellet, C., Pelto, M.S., Perkins-Kirkpatrick, S.E., Petron, G., Phillips, C., Po-Chedley, S., Polvani, L., Preimesberger, W., Rains, D.G., Randel, W.J., Rayner, N. A., Rémy, S., Ricciardulli, L., Richardson, A.D., Robinson, D.A., Rodell, M., Rodríguez-Fernández, N.J., Rosenlof, K.H., Roth, C., Rozanov, A., Rutishäuser, T., Sánchez-Lugo, A., Sawaengphokhai, P., Scanlon, T., Schenzinger, V., Schlegel, R.W., Sharma, S., Shi, L., Simmons, A.J., Siso, C., Smith, S.L., Soden, B.J., Sofieva, V., Sparks, T.H., Stackhouse, P.W., Steinbrecht, W., Stengel, M., Streletskiy, D.A., Sun-Mack, S., Tans, P., Thackeray, S.J., Thibert, E., Tokuda, D., Tourpali, K., Tye, M.R., Schalie, R., Schrier, G., Vliet, M., Werf, G.R., Vance, A., Vernier, J.-P., Vimont, I.J., Vömel, H., Vose, R.S., Wang, R., Weber, M., Wiese, D., Wilber, A.C., Wild, J.D., Wong, T., Woolway, R.I., Zhou, X., Yin, X., Zhao, G., Zhao, L., Ziemke, J.R., Ziese, M., Zotta, R.M., 2021. Global climate. Bull. Am. Meteorol. Soc. 102, S11–S142. https://doi.org/10.1175/BAMS-D-21-0098.1.

Estiarte, M., Peñuelas, J., 2015. Alteration of the phenology of leaf senescence and fall in winter deciduous species by climate change: effects on nutrient proficiency. Glob. Chang Biol. 21, 1005–1017. https://doi.org/10.1111/gcb.12804.

Fracheboud, Y., Luquez, V., Björkén, L., Sjödin, A., Tuominen, H., Jansson, S., 2009. The control of autumn senescence in European Aspen. Plant Physiol. 149, 1982–1991. https://doi.org/10.1104/pp.108.133249.

Friedl, M.A., 2021. MuSLI multi-source land surface phenology yearly North America 30m V011. Distributed by NASA EOSDIS Land Processes DAAC. 10.5067/Community/MuSLI/MSLSP30NA.011.

Friedman, J.M., Roelle, J.E., Cade, B.S., 2011. Genetic and environmental influences on leaf phenology and cold hardiness of native and introduced riparian trees. Int. J. Biometeorol. 55, 775–787. https://doi.org/10.1007/s00484-011-0494-6.

Fu, Y.H., Piao, S., Delpierre, N., Hao, F., Hänninen, H., Liu, Y., Sun, W., Janssens, I.A., Campioli, M., 2018. Larger temperature response of autumn leaf senescence than spring leaf-out phenology. Glob. Change Biol. 24, 2159–2168. https://doi.org/10.1111/gcb.14021.

Gallinat, A.S., Primack, R.B., Wagner, D.L., 2015. Autumn, the neglected season in climate change research. Trends Ecol. Evol. 30, 169–176. https://doi.org/10.1016/j.tree.2015.01.004.

Gao, F., Anderson, M.C., Zhang, X., Yang, Z., Alfieri, J.G., Kustas, W.P., Mueller, R., Johnson, D.M., Prueger, J.H., 2017. Toward mapping crop progress at field scales through fusion of Landsat and MODIS imagery. Remote Sens. Environ. 188, 9–25. https://doi.org/10.1016/j.rse.2016.11.004.

Gill, A.L., Gallinat, A.S., Sanders-DeMott, R., Rigden, A.J., Short Gianotti, D.J., Mantooth, J.A., Templer, P.H., 2015. Changes in autumn senescence in northern hemisphere deciduous trees: a meta-analysis of autumn phenology studies. Ann. Bot. 116, 875–888. https://doi.org/10.1093/aob/mcv055.

Hänninen, H., Kramer, K., Tanino, K., Zhang, R., Wu, J., Fu, Y.H., 2019. Experiments are necessary in process-based tree phenology modelling. Trends Plant Sci. 24, 199–209. https://doi.org/10.1016/j.tplants.2018.11.006.

Havé, M., Marmagne, A., Chardon, F., Masclaux-Daubresse, C., 2017. Nitrogen remobilization during leaf senescence: lessons from Arabidopsis to crops. J. Exp. Bot. 68, 2513–2529. https://doi.org/10.1093/jxb/erw365.

Hemmerling, J., Pflugmacher, D., Hostert, P., 2021. Mapping temperate forest tree species using dense Sentinel-2 time series. Remote Sens. Environ. 267, 112743 https://doi.org/10.1016/j.rse.2021.112743.

Jiang, Z., Huete, A.R., Didan, K., Miura, T., 2008. Development of a two-band enhanced vegetation index without a blue band. Remote Sens. Environ. 112, 3833–3845. https://doi.org/10.1016/j.rse.2008.06.006.

Keenan, T.F., Darby, B., Felts, E., Sonnentag, O., Friedl, M.A., Hufkens, K., O'Keefe, J., Klosterman, S., Munger, J.W., Toomey, M., Richardson, A.D., 2014. Tracking forest phenology and seasonal physiology using digital repeat photography: a critical assessment. Ecol. Appl. 24, 1478–1489. https://doi.org/10.1890/13-0652.1.

Keenan, T.F., Richardson, A.D., 2015. The timing of autumn senescence is affected by the timing of spring phenology: implications for predictive models. Glob. Chang Biol. 21, 2634–2641. https://doi.org/10.1111/gcb.12890.

Keskitalo, J., Bergquist, G., Gardeström, P., Jansson, S., 2005. A cellular timetable of autumn senescence. Plant Physiol. 139, 1635–1648. https://doi.org/10.1104/pp.105.066845.

Lang, W., Chen, X., Qian, S., Liu, G., Piao, S., 2019. A new process-based model for predicting autumn phenology: how is leaf senescence controlled by photoperiod and temperature coupling? Agric. For. Meteorol. 268, 124–135. https://doi.org/10.1016/j.agrformet.2019.01.006.

Leuzinger, S., Luo, Y., Beier, C., Dieleman, W., Vicca, S., Körner, C., 2011. Do global change experiments overestimate impacts on terrestrial ecosystems? Trends Ecol. Evol. 26, 236–241. https://doi.org/10.1016/j.tree.2011.02.011.

Liu, Q., Piao, S., Campioli, M., Gao, M., Fu, Y.H., Wang, K., He, Y., Li, X., Janssens, I.A., 2020. Modeling leaf senescence of deciduous tree species in Europe. Glob. Chang Biol. 26, 4104–4118. https://doi.org/10.1111/gcb.15132.

Mann, H.B., 1945. Nonparametric tests against trend. Econometrica 13, 245–259. https://doi.org/10.2307/1907187.

Meng, L., Zhou, Y., Li, X., Asrar, G.R., Mao, J., Wanamaker, A.D., Wang, Y., 2020. Divergent responses of spring phenology to daytime and nighttime warming. Agric. For. Meteorol. 281, 107832 https://doi.org/10.1016/j.agrformet.2019.107832.

Moon, M., Li, D., Liao, W., Rigden, A.J., Friedl, M.A., 2020. Modification of surface energy balance during springtime: the relative importance of biophysical and meteorological changes. Agric. For. Meteorol. 284, 107905 https://doi.org/10.1016/j.agrformet.2020.107905.

Moon, M., Richardson, A.D., Friedl, M.A., 2021a. Multiscale assessment of land surface phenology from harmonized Landsat 8 and Sentinel-2, PlanetScope, and PhenoCam imagery. Remote Sens. Environ. 266, 112716 https://doi.org/10.1016/j.rse.2021.112716.

Moon, M., Seyednasrollah, B., Richardson, A.D., Friedl, M.A., 2021b. Using time series of MODIS land surface phenology to model temperature and photoperiod controls on spring greenup in North American deciduous forests. Remote Sens. Environ. 260, 112466 https://doi.org/10.1016/j.rse.2021.112466.

Munger, W., Wofsy, S., 2020. Canopy-atmosphere exchange of carbon, water and energy at Harvard forest EMS tower since 1991. Harvard Forest Data Archive: HF004 (v.32). 10.6073/pasta/6e1e3d902387781c1d9822cce8444ede.

Nelder, J.A., Mead, R., 1965. A simplex method for function minimization. Comput. J. 7, 308–313. https://doi.org/10.1093/comjnl/7.4.308.

O'Keefe, J., 2019. Phenology of woody species at Harvard forest since 1990. Harvard Forest Data Archive: HF003. 10.6073/pasta/91e3b7c2548a0f2e251729eeacbce312.

Park, T., Ganguly, S., Tømmervik, H., Euskirchen, E.S., Høgda, K.-A., Karlsen, S.R., Brovkin, V., Nemani, R.R., Myneni, R.B., 2016. Changes in growing season duration and productivity of northern vegetation inferred from long-term remote sensing data. Environ. Res. Lett. 11, 084001 https://doi.org/10.1088/1748-9326/11/8/084001.

Peano, D., Hemming, D., Materia, S., Delire, C., Fan, Y., Joetzjer, E., Lee, H., Nabel, J.E. M.S., Park, T., Peylin, P., Wårlind, D., Wiltshire, A., Zaehle, S., 2021. Plant phenology evaluation of CRESCENDO land surface models – Part 1: start and end of the growing season. Biogeosciences 18, 2405–2428. https://doi.org/10.5194/bg-18-2405-2021.

Peng, J., Wu, C., Wang, X., Lu, L., 2021. Spring phenology outweighed climate change in determining autumn phenology on the Tibetan Plateau. Int. J. Climatol. 41, 3725–3742. https://doi.org/10.1002/joc.7045.

Peng, J., Wu, C., Zhang, X., Wang, X., Gonsamo, A., 2019. Satellite detection of cumulative and lagged effects of drought on autumn leaf senescence over the Northern Hemisphere. Glob. Change Biol. 25, 2174–2188. https://doi.org/10.1111/gcb.14627.

Piao, S., Liu, Q., Chen, A., Janssens, I.A., Fu, Y., Dai, J., Liu, L., Lian, X., Shen, M., Zhu, X., 2019. Plant phenology and global climate change: current progresses and challenges. Glob. Change Biol. https://doi.org/10.1111/gcb.14619.

Primack, R.B., Laube, J., Gallinat, A.S., Menzel, A., 2015. From observations to experiments in phenology research: investigating climate change impacts on trees and shrubs using dormant twigs. Ann. Bot. 116, 889–897. https://doi.org/10.1093/aob/mcv032.

Reichstein, M., Camps-Valls, G., Stevens, B., Jung, M., Denzler, J., Carvalhais, N., Prabhat, 2019. Deep learning and process understanding for data-driven Earth system science. Nature 566, 195. https://doi.org/10.1038/s41586-019-0912-1.

Renner, S.S., Zohner, C.M., 2018. Climate change and phenological mismatch in trophic interactions among plants, insects, and vertebrates. Annu. Rev. Ecol. Evol. Syst. 49, 165–182. https://doi.org/10.1146/annurev-ecolsys-110617-062535.

Richardson, A.D., Anderson, R.S., Arain, M.A., Barr, A.G., Bohrer, G., Chen, G., Chen, J. M., Ciais, P., Davis, K.J., Desai, A.R., Dietze, M.C., Dragoni, D., Garrity, S.R., Gough, C.M., Grant, R., Hollinger, D.Y., Margolis, H.A., McCaughey, H., Migliavacca, M., Monson, R.K., Munger, J.W., Poulter, B., Raczka, B.M., Ricciuto, D. M., Sahoo, A.K., Schaefer, K., Tian, H., Vargas, R., Verbeeck, H., Xiao, J., Xue, Y., 2012. Terrestrial biosphere models need better representation of vegetation phenology: results from the North American Carbon Program Site Synthesis. Glob. Change Biol. 18, 566–584. https://doi.org/10.1111/j.1365-2486.2011.02562.x.

Richardson, A.D., Bailey, A.S., Denny, E.G., Martin, C.W., O'keefe, J., 2006. Phenology of a northern hardwood forest canopy. Glob. Change Biol. 12, 1174–1188. https://doi.org/10.1111/j.1365-2486.2006.01164.x.

Richardson, A.D., Hufkens, K., Milliman, T., Aubrecht, D.M., Furze, M.E., Seyednasrollah, B., Krassovski, M.B., Latimer, J.M., Nettles, W.R., Heiderman, R.R., Warren, J.M., Hanson, P.J., 2018. Ecosystem warming extends vegetation activity but heightens vulnerability to cold temperatures. Nature. https://doi.org/10.1038/s41586-018-0399-1.

Schaber, J., Badeck, F.-W., 2003. Physiology-based phenology models for forest tree species in Germany. Int. J. Biometeorol. 47, 193–201. https://doi.org/10.1007/s00484-003-0171-5.

Sen, P.K., 1968. Estimates of the regression coefficient based on Kendall's Tau. J. Am. Stat. Assoc. 63, 1379–1389. https://doi.org/10.2307/2285891.

Su, Y.-S., Yajima, M., 2015. R2jags: Using R to Run "JAGS". R package version 0.5-7 34.

USGS, Rigge, M., 2019. National Land Cover Database (NLCD) 2016 Shrubland Fractional Components for the Western U.S. (ver. 3.0, July 2020). U.S. Geological Survey data release. https://doi.org/10.5066/P9MJVQSQ.

Vitasse, Y., Baumgarten, F., Zohner, C.M., Kaewthongrach, R., Fu, Y.H., Walde, M.G., Moser, B., 2021. Impact of microclimatic conditions and resource availability on spring and autumn phenology of temperate tree seedlings. New Phytol. nph 17606. https://doi.org/10.1111/nph.17606.

Vitasse, Y., Lenz, A., Hoch, G., Körner, C., 2014. Earlier leaf-out rather than difference in freezing resistance puts juvenile trees at greater risk of damage than adult trees. J. Ecol. 102, 981–988. https://doi.org/10.1111/1365-2745.12251.

Wilson, B., Lister, A.J., Riemann, R.I., Griffith, D.M., 2013. Live tree species basal area of the contiguous United States (2000-2009). Newtown Square, PA: USDA Forest Service. Rocky Mountain Res. Station. https://doi.org/10.2737/RDS-2013-0013.

Wolkovich, E.M., Cook, B.I., Allen, J.M., Crimmins, T.M., Betancourt, J.L., Travers, S.E., Pau, S., Regetz, J., Davies, T.J., Kraft, N.J.B., Ault, T.R., Bolmgren, K., Mazer, S.J., McCabe, G.J., McGill, B.J., Parmesan, C., Salamin, N., Schwartz, M.D., Cleland, E.E.,

2012. Warming experiments underpredict plant phenological responses to climate change. Nature 485, 494–497. https://doi.org/10.1038/nature11014.

Wu, C., Wang, X., Wang, H., Ciais, P., Peñuelas, J., Myneni, R.B., Desai, A.R., Gough, C. M., Gonsamo, A., Black, A.T., Jassal, R.S., Ju, W., Yuan, W., Fu, Y., Shen, M., Li, S., Liu, R., Chen, J.M., Ge, Q., 2018. Contrasting responses of autumn-leaf senescence to daytime and night-time warming. Nat. Clim. Change 8, 1092. https://doi.org/10.1038/s41558-018-0346-z.

Xie, Y., Wang, X., Wilson, A.M., Silander, J.A., 2018. Predicting autumn phenology: how deciduous tree species respond to weather stressors. Agric. For. Meteorol. 250–251, 127–137. https://doi.org/10.1016/j.agrformet.2017.12.259.

Xu, X., Riley, W.J., Koven, C.D., Jia, G., Zhang, X., 2020. Earlier leaf-out warms air in the north. Nat. Clim. Change 10, 370–375. https://doi.org/10.1038/s41558-020-0713-4.

Young, A.M., Friedl, M.A., Seyednasrollah, B., Beamesderfer, E., Carrillo, C.M., Li, X., Moon, M., Arain, M.A., Baldocchi, D.D., Blanken, P.D., Bohrer, G., Burns, S.P., Chu, H., Desai, A.R., Griffis, T.J., Hollinger, D.Y., Litvak, M.E., Novick, K., Scott, R.L., Suyker, A.E., Verfaillie, J., Wood, J.D., Richardson, A.D., 2021. Seasonality in aerodynamic resistance across a range of North American ecosystems. Agric. For. Meteorol. 310, 108613 https://doi.org/10.1016/j.agrformet.2021.108613.

Zani, D., Crowther, T.W., Mo, L., Renner, S.S., Zohner, C.M., 2020. Increased growing-season productivity drives earlier autumn leaf senescence in temperate trees. Science 370, 1066–1071. https://doi.org/10.1126/science.abd8911.

Zhang, S., Dai, J., Ge, Q., 2020a. Responses of autumn phenology to climate change and the correlations of plant hormone regulation. Sci. Rep. 10, 9039. https://doi.org/10.1038/s41598-020-65704-8.

Zhang, Y., Commane, R., Zhou, S., Williams, A.P., Gentine, P., 2020b. Light limitation regulates the response of autumn terrestrial carbon uptake to warming. Nat. Clim. Change 1–5. https://doi.org/10.1038/s41558-020-0806-0.

Zohner, C.M., Benito, B.M., Svenning, J.-C., Renner, S.S., 2016. Day length unlikely to constrain climate-driven shifts in leaf-out times of northern woody plants. Nat. Clim. Change 6, 1120–1123. https://doi.org/10.1038/nclimate3138.